

Article

A Study on the Mechanism of Casing Deformation and Its Control Strategies in Shale Oil Hydraulic Fracturing

Nan Zhang ^{1,2,*}, Peng Wang ^{1,2}, Junliang Li ^{1,2}, Wenhai Ma ^{1,2}, Xiaochuan Zhang ^{1,2}, Hongtao Zhang ^{1,2}, Chenggang Jiang ^{1,2}, Weiming Huang ^{1,2}, Xinzhu Feng ^{1,2} and Shuwei Liu ^{1,2}

¹ Daqing Oil Field Production Technology Institute, Daqing 163000, China

² Heilongjiang Provincial Key Laboratory of Oil and Gas Reservoir Stimulation, Daqing 163000, China

* Correspondence: zhangnanhw@petrochina.com.cn; Tel.: +86-0459-5960052

Abstract: The problem of casing deformation caused by large-scale hydraulic fracturing in shale oil wells severely restricts the efficient development of Gulong shale oil. In order to clarify the mechanism of casing deformation in shale oil wells, comprehensive analysis was conducted on engineering factors, multi-arm caliper logging, seismic attributes, and the distribution characteristics of casing deformations. This study shows that casing strength, cementing quality, and wellbore curvature are not the main controlling factors for casing deformation. Casing deformation is caused by the communication between hydraulic fractures and natural fractures during the fracturing process, which increases the fluid pressure in the natural fracture and induces shear slip, resulting in casing deformation due to shear stress. Based on the understanding of the mechanism of casing deformation in shale oil wells, two targeted casing deformation prevention and control methods are proposed. First, temporary plugging was implemented during the hydraulic fracturing process when the fluid volume reached 1000 m³, and the pumping rate was reduced to below 16 m³/min to reduce the internal fluid pressure of the fractures and control fracture slip, thereby minimizing the risk of casing deformation. Second, hollow particles were added to the cement to enhance the consolidation effect of the cement sheath and mitigate casing deformation caused by fracture slip. Research indicates that a hollow particle content of 15% can meet the requirements for casing deformation control in Gulong shale oil. These research results can provide important references for the prediction and prevention of casing deformation risks in shale oil and similar unconventional reservoirs during hydraulic fracturing.

Keywords: shale oil; hydraulic fracturing; casing deformation; fracture slip; prevention of casing deformation



Citation: Zhang, N.; Wang, P.; Li, J.; Ma, W.; Zhang, X.; Zhang, H.; Jiang, C.; Huang, W.; Feng, X.; Liu, S. A Study on the Mechanism of Casing Deformation and Its Control Strategies in Shale Oil Hydraulic Fracturing. *Processes* **2023**, *11*, 2437. <https://doi.org/10.3390/pr11082437>

Academic Editors: Xinhong Li, Shangyu Yang and Huixing Meng

Received: 6 July 2023

Revised: 6 August 2023

Accepted: 9 August 2023

Published: 13 August 2023



Copyright: © 2023 by the authors. Licensee MDPI, Basel, Switzerland. This article is an open access article distributed under the terms and conditions of the Creative Commons Attribution (CC BY) license (<https://creativecommons.org/licenses/by/4.0/>).

1. Introduction

Shale oil and other unconventional oil and gas resources are an important area for the strategic replacement of oil and gas resources in China. Major domestic oilfields have gradually expanded their shale oil and gas development. However, due to the tightness of shale reservoirs, massive fracturing transformation is required to achieve effective utilization. Deformation of the casing often occurs during the large-scale fracturing process of shale oil and gas wells. In the Changning and Weiyuan blocks of the Southwest oil and gas fields, the casing deformation rate in shale gas wells reached 35.6%, and serious casing deformation issues also existed in the development process of shale reservoirs, such as the Jimusaer shale oil in Xinjiang [1,2]. Casing deformation results in the inability to position subsequent bridge plugs accurately during construction and causes blockages during subsequent drilling. Severe casing deformations in some sections lead to the abandonment of layers. The deformation of the casing not only directly leads to a decrease in the number of fracturing stages and a decline in production but also causes integrity issues in the wellbore, thereby shortening the life of the well and significantly reducing the ultimate recovery rate, which severely restricts the efficient and economical development

of shale oil and gas. In recent years, the exploration and development of shale oil in the Gulong area of Daqing have also entered the exploration and development stage. However, the problem of casing deformations causing blockages during the fracturing process has been observed; in the test area, the casing deformation rate in the horizontal wells reached 16.7%, which severely affected the development efficiency of the shale oil. Some domestic and foreign scholars have conducted research on casing deformation in horizontal wellbore shale reservoirs. Shen, Jiang Ke, and others have proposed that the casing stress concentration caused by uneven fracturing transformation and poor cementing quality is the main factor leading to casing deformation [3,4]. Yu Hao and others believe that the asymmetric fracturing transformation and changes in near-wellbore stress increase the uneven distribution of casing stress, leading to casing deformation [5,6]. Fan Mingtao and others believe that the injection of a large amount of fracturing fluid during the fracturing process can cause significant temperature differences, which is an important factor in casing deformation [7–9]. In recent years, Chen Chaowei, Li Liuwei, and others have proposed that casing deformation in shale gas wells is caused by the initiation of pre-existing fractures during the fracturing process, resulting in a shear slip of the formation on both sides of the fracture and casing deformation [10–17]. Based on the above analyses, it is clear that there is still no unified understanding of the mechanism of casing deformation during large-scale hydraulic fracturing in shale reservoirs. Therefore, further in-depth research is needed to understand the mechanism and control measures for casing deformation in shale oil wells, taking into account the geological and engineering parameters related to casing deformation in the field.

The Gulong shale oil reserves are enormous and are an important replacement resource for the Daqing Oilfield. Improving the effectiveness of fracturing through casing deformation prevention and control not only has practical economic benefits but also holds significant strategic importance. This article analyzes the deformation mechanism of casings in the Daqing Gulong shale oil fracturing test area based on data such as casing strength, cementing quality, multi-arm caliper diameter logging, and seismic attributes. It proposes targeted measures for casing deformation prevention and control, providing theoretical guidance for risk prediction and prevention of casing deformation.

2. Analysis of the Casing Deformation Mechanism

2.1. Analysis of the Impact of Casing Strength on Casing Deformation

Shale oil well fracturing operations involve large volumes and high pressures. When the pressure exceeds the strength of the casing, it can cause deformation. For the Gulong shale oil horizontal wells, Q125-grade steel with a wall thickness of 10.54 mm is used for the casing. Through the mechanical analysis of the pipe string, the stress of the casing under different fracturing rates was analyzed. The results showed that at a pumping pressure of 75 MPa and a rate of 18 m³/min, the casing had a safety factor of 1.6 or greater. Additionally, fatigue experiments were conducted on the casing under cyclic loads to analyze the impact on strength reduction caused by multistage fracturing. The experiments showed that the strength of the Q125 casing only decreased by 7% after 50 cycles of internal pressure of 100 MPa. Under the conditions of fracturing, the casing still maintained a safety factor of 1.5 or greater, as shown in Figure 1. Therefore, from the analysis of casing strength, casing deformation does not occur during fracturing.

2.2. Analysis of the Impact of Cementing Quality on Casing Deformation

During the cementing process of a horizontal well, the cement slurry is prone to segregation in the vertical direction due to the influence of gravity, resulting in local voids in the cement sheath after solidification, which leads to stress concentration in the casing and causes casing deformation during fracturing. The casing-cement sheath-formation static mechanical coupling model was established using ABAQUS finite element simulation software to analyze the stress state of a casing of Q125-grade steel, with a 139.7 mm diameter and 10.54 mm wall thickness, under the condition of a missing angle of 30° in the cement

annulus. The model was divided by hexahedral meshes, adopting the Von Mises yield criterion and simplifying the casing, cement sheath, and formation as homogeneous and isotropic materials. Other parameters of the model are shown in Table 1.

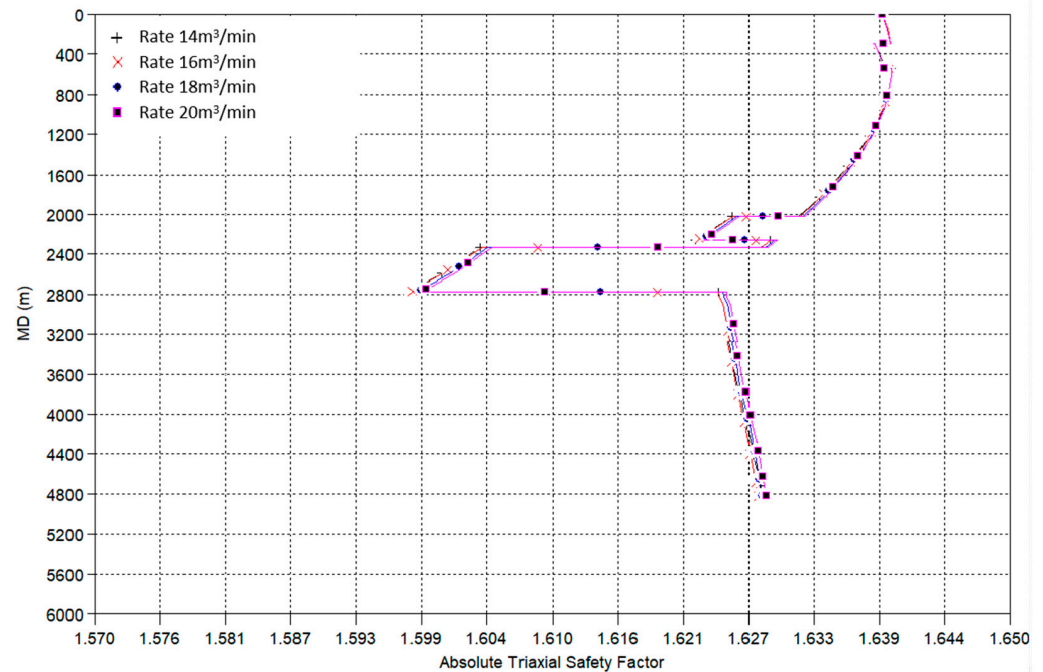


Figure 1. Analysis of the triaxial safety factor of casing under different rates of fracturing.

Table 1. The parameters of the simulation model of casing stress analysis.

Parameters of casing	
Young's modulus	210 GPa
Poisson's ratio	0.3
Outside diameter	139.7
Thickness	10.54
Parameters of cement sheath	
Young's modulus	7 GPa
Poisson's ratio	0.2
Thickness	38.1 mm
Parameters of rock	
Young's modulus	20 GPa
Poisson's ratio	0.2

The results show that when the cement sheath has voids, the increase in differential stress leads to a significant increase in the equivalent stress on the casing. The maximum equivalent stresses on the casing were 425 MPa, 559 MPa, 694 MPa, and 818 MPa, respectively, for differential stresses of 0 MPa, 10 MPa, 20 MPa, and 30 MPa, as shown in Figure 2. However, it still did not reach the rated yield strength of the casing, which was 864 MPa. Meanwhile, analysis of the relationship between bridge plugging points and cementing quality in the Gulong shale oil test area showed that the cementing quality was mainly good when encountering bridge plugging points, with 61 out of 74 bridge plugs having good cementing quality, accounting for 82.4%. Therefore, it is concluded that poor cementing quality is not the primary controlling factor for casing deformation.

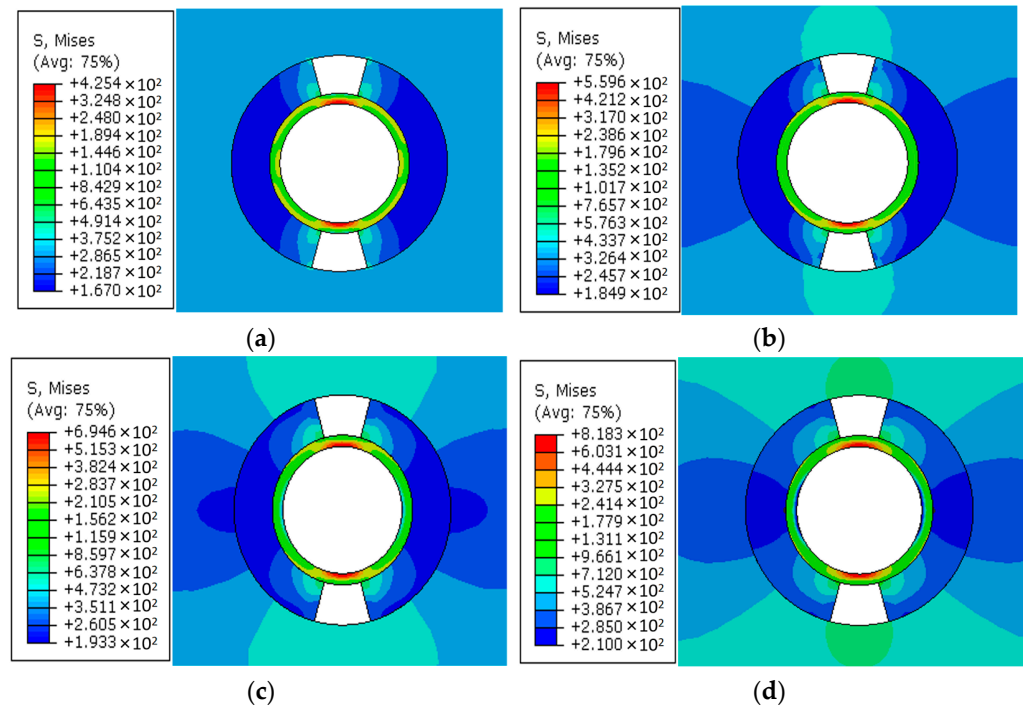


Figure 2. Variation in casing stress under different ground stress differences: (a) differential stress of 0 MPa; (b) differential stress of 10 MPa; (c) differential stress of 20 MPa; (d) differential stress of 30 MPa.

2.3. Analysis of the Impact of Wellbore Curvature on Casing Deformation

When the local curvature of the wellbore trajectory in a horizontal well is high, bending of the casing can lead to stress concentration and increase the risk of casing deformation. However, statistical analysis of the wellbore curvature at the points where bridge plugs encounter resistance showed that the wellbore trajectory at these points was generally low. In fact, 83.8% of these points had a curvature of less than $2^\circ/30\text{ m}$, as shown in Figure 3. This indicates that there is not a close relationship between the bridge plugs' resistance and casing deformation. The risk of casing deformation caused by stress concentration due to bending is relatively low. Therefore, the wellbore curvature is not the main factor affecting casing deformation.

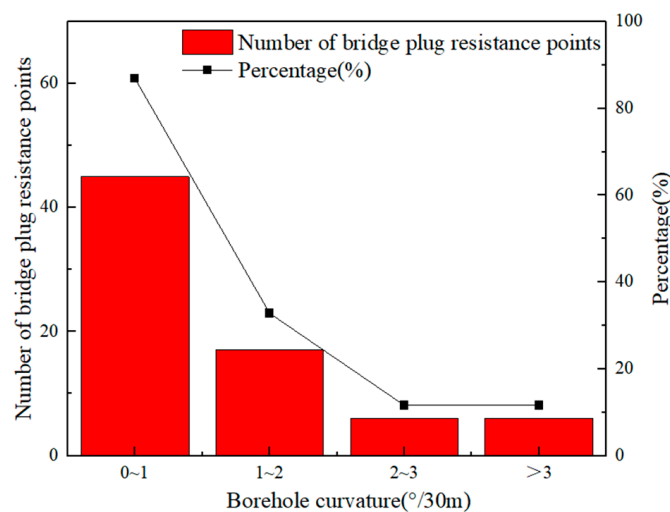


Figure 3. Wellbore curvature statistics of drilling plugs in shale oil wells.

2.4. Analysis of the Morphological Characteristics of Casing Deformation

Multi-arm caliper logging can directly reflect the characteristics of casing deformation through changes in the casing's inner diameter. It is the most direct and accurate method to analyze casing deformation morphology. The analysis of multi-arm caliper logging in the Gulong shale oil test area indicated that the morphology of casing deformations at the deformation zone often exhibited an S-shaped feature, indicating asymmetric compression caused by shear deformation. Taking the casing deformation location of well SY2-3 as an example, the interpretation of the cross-section using multi-arm caliper logging showed an eccentric elliptical shape, and the casing had obvious S-shaped shear displacement features in the three-dimensional image, as shown in Figure 4. Additionally, the analysis of lead molds after casing transformation in well A34 in the test area also showed a crescent-shaped cutting on one side and no change on the other side, indicating shear deformation, as shown in Figure 5. Therefore, the analysis of the deformation features of the casings in the Gulong shale oil wells indicated that the deformation of the casings was a shear deformation caused by shear forces. Generally speaking, the shear deformation of the casing is related to sliding along weak planes in the formation. In the test area of the Gulong shale oil, the fractures were well-developed. Based on the deformation features of the casing, it was preliminarily analyzed that the deformation of the casings was caused by the shear and slip of the casing due to fractures. To validate this analysis, a finite element model of casing-cement-formation with pre-existing fractures was established to simulate the effect of fracture slip on casing deformation. The model set the fracture inclination angle to 75° . The casing, cement sheath, and formation were simplified as homogeneous and isotropic materials, and the model used hexahedral mesh division. Other parameters of the model are shown in Table 2. The analysis showed that when there was a fracture slip, the casing underwent shear deformation, and the deformation features were consistent with the deformation features observed in well logging, as shown in Figure 6. This also provides preliminary confirmation of the analysis of the casing deformation mechanism.

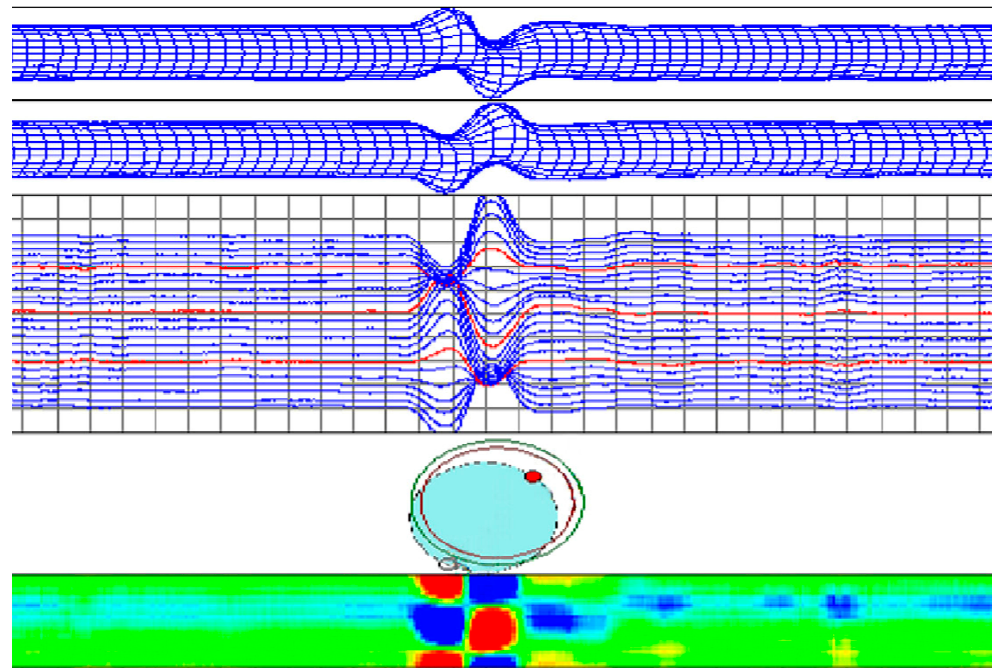


Figure 4. Multi-arm caliper logging interpretation of SYQ2-3.



Figure 5. Lead seal morphology features of A34.

Table 2. The parameters of the simulation model of casing shear deformation.

Parameters of casing	
Young's modulus	210 GPa
Poisson's ratio	0.3
Outside diameter	139.7
Thickness	10.54
Parameters of cement sheath	
Young's modulus	7 GPa
Poisson's ratio	0.2
Thickness	38.1 mm
Parameters of rock	
Young's modulus	20 GPa
Poisson's ratio	0.2
Parameters of fracture	
Dip	75°

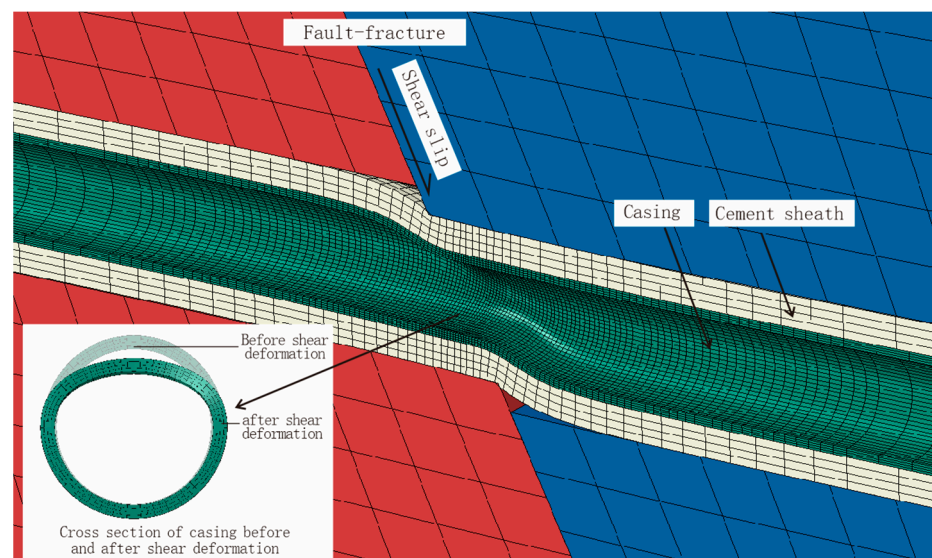


Figure 6. Finite element simulation results of fracture shear slip leading to casing deformation.

2.5. Fracture Stability Analysis

Natural fractures are mechanical weak planes in the formations, where they are more prone to failure compared to the surrounding rock under the same stress conditions. In

order to assess the activity of pre-existing fractures during hydraulic fracturing processes, previous studies have further developed a generalized shear activity criterion based on the classical Mohr–Coulomb failure criterion [18,19]. This criterion quantitatively evaluates the possibility of fracture activity under different geostress fields, fluid pressures, and fracture attitudes [20]. A schematic diagram of the generalized shear activity criterion is shown in Figure 7, and its mathematical expression is shown in Equation (1) [21], where f_a is the fracture activity coefficient, which represents the ratio of the actual shear stress acting on the fracture surface to the critical shear stress required for a fracture to occur. When $f_a < 1.0$, the fracture is in a stable state; when $f_a = 1.0$, the fracture is in a critical active state; when $f_a > 1.0$, the fracture will experience shear activity; and a higher value of f_a indicates a higher risk of fracture activity.

$$f_a = \frac{\sqrt{\sigma_1^2 \sin 2\theta + \sigma_2^2 \cos 2\theta \cos 2\alpha + \sigma_3^2 \cos 2\theta \sin 2\alpha - (\sigma_1 \sin 2\theta + \sigma_2 \cos 2\theta \cos 2\alpha + \sigma_3 \cos 2\theta \sin 2\alpha)^2}}{C + \mu(\sigma_1^2 \sin 2\theta + \sigma_2^2 \cos 2\theta \cos 2\alpha + \sigma_3^2 \cos 2\theta \sin 2\alpha - P)} \quad (1)$$

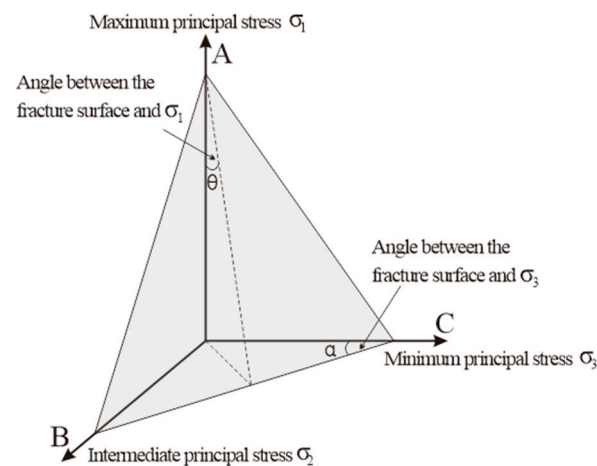


Figure 7. Diagram of generalized shear failure criteria.

In the formula:

σ_1 is the maximum principal stress, MPa;

σ_2 is the intermediate principal stress, MPa;

σ_3 is the minimum principal stress, MPa;

θ is the angle between the fracture surface and σ_1 , °;

α is the angle between the fracture surface and σ_3 , °;

C is the cohesion of the fracture surface, MPa;

μ is the friction coefficient of the fracture, dimensionless;

P is the fluid pressure, MPa.

From the analysis of the expression of the generalized shear activity criterion, it can be seen that the occurrence of fracture activity is mainly controlled by the geostress field, fracture attitude, cohesive strength, and fluid pressure within the fracture plane. The first three parameters can generally be considered constant under specific geological conditions. Therefore, the fluid pressure within the fracture plane is the main controlling factor affecting fracture activity. When hydraulic fracturing creates a connection between artificial fractures and pre-existing fractures, it increases the fluid pressure within the fracture plane, thereby inducing fracture activity.

In addition, the generalized shear activity theory can also be visually expressed using Mohr circles; the abscissa represents the normal stress acting on the fracture plane, the ordinate represents the shear stress acting on the fracture plane, and the inclined line represents the critical activity line for a fracture. When hydraulic fractures communicate with pre-existing fractures and cause an increase in fluid pressure within the fracture plane, the normal stress σ_n on the fracture plane decreases, and the Mohr circle moves to the left.

When it crosses the critical activity line (i.e., when $f_a > 1.0$ in Equation (1)), the fracture undergoes shear sliding. Based on the generalized shear activity criterion and the geostress field data of the SY shale oil test area, the activity of 32 identified fractures was analyzed. The analysis results indicated that the fractures were in a stable state under the original fluid pressure conditions. However, during hydraulic fracturing, when the fluid pressure within the fracture plane increased to the minimum principal stress level, the fracture activity coefficient f_a was greater than 1 for most fractures, indicating that the fractures would be activated and undergo shear sliding, as shown in Figure 8.

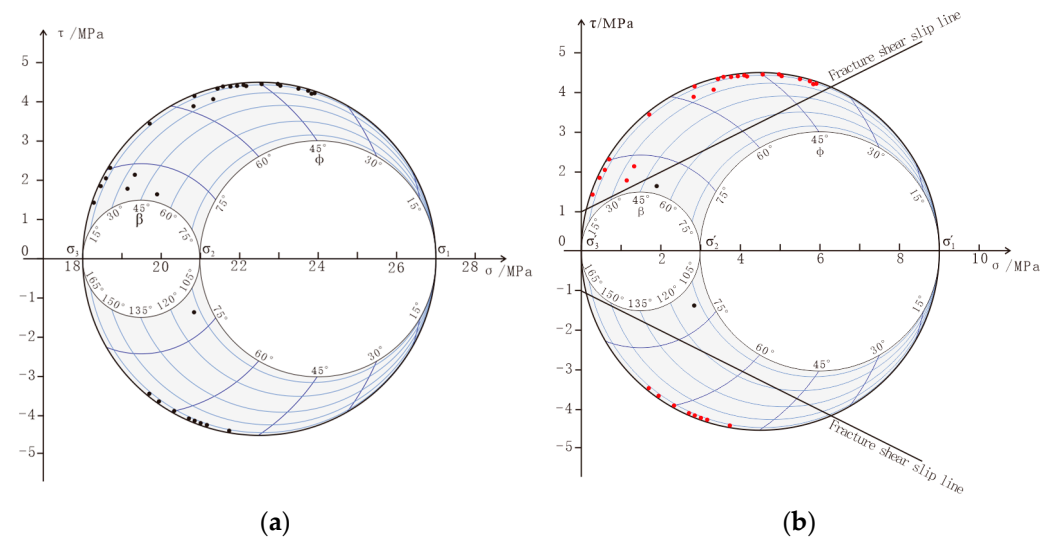


Figure 8. Fracture activity analysis before and after fracturing in SY test area: (a) analysis of fracture activity before fracturing; (b) analysis of fracture activity after fracturing.

2.6. The Correlation between the Distribution of Casing Deformation Points and Fractures

To further verify the casing deformation mechanism induced by hydraulic fracturing, the relationship between the distribution of casing deformation points and the location of the fractures was analyzed. Generally, the combination of seismic and amplitude attributes can better reflect the location of a fracture. According to the analysis of the distribution characteristics of the fractures in the SY test area identified through geological identification and the bridge plug resistance points of horizontal wells in this area, it was concluded that the bridge plug resistance points were closely related to the location of the fractures; most of the bridge plug resistance points were distributed near the predicted fractures, accounting for 71.9%, as shown in Figure 9. This further confirms that the casing deformation mechanism is caused by the fracture sliding and the shearing of the casing which are induced by hydraulic fracturing.

Based on the analysis of various factors mentioned above, it is believed that the casing deformation mechanism in the Gulong shale oil formation is the communication between hydraulic fractures and pre-existing fractures during the fracturing process. After the fracturing fluid enters the fracture surface, it induces fracture sliding, resulting in deformation of the casing.

However, it should be noted that although the distribution of fractures and the casing deformations predicted based on seismic data shows a high degree of agreement, it still cannot accurately reflect all the locations of casing deformation. This analysis may be related to the accuracy of seismic data. Therefore, it is recommended to conduct a fine identification of fractures within the wellbore based on drilling and logging data to further verify the casing deformation mechanism and improve the accuracy of casing deformation risk prediction.

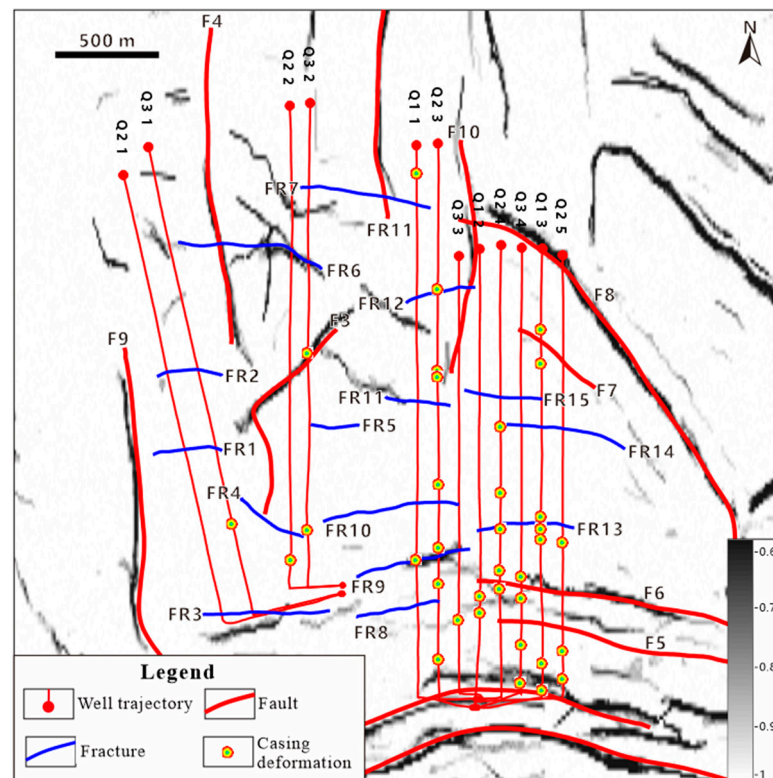


Figure 9. Map of the distribution of casing deformations and fractures in the SY test area.

3. Risk Prevention and Control Measures for Casing Deformation

Based on the understanding of the casing deformation mechanism of Gulong shale oil, the following two concepts for preventing and controlling casing deformation are proposed to reduce the risk of casing deformation during fracturing process. First, the fundamental measure for preventing and controlling casing deformation is to control the fluid pressure within the fracture surface during the fracturing process, reducing the risk of fracture slip. Second, a new type of cement system should be used to absorb the displacement of the fracture slip when hydraulic fracturing induces fracture slip and shears the wellbore, thereby reducing casing deformation. Based on the above analysis, a set of casing deformation prevention and control methods were designed, focusing on optimizing the timing of temporary plugging and pumping rates during fracturing, and optimizing the cement system.

3.1. Casing Deformation Prevention and Control Method Based on Temporary Plugging and Pumping Rate Optimization

3.1.1. Theoretical Analysis of Casing Deformation Prevention and Control through Temporary Plugging

During hydraulic fracturing in shale oil, there are only two flow paths for fracturing fluid: one is the flow along the hydraulic fracture, and the other is the flow along pre-existing natural fractures. The goal of fracturing is to create fractures along the hydraulic fracture, while if the fracturing fluid flows along the fracture, it not only reduces the effectiveness of fracturing but also induces fracture slip, leading to casing deformation. Previous studies have shown that the ability of fluids to flow along different types of fractures is closely related to the scale of the fractures under the conditions of geostress, which can be expressed by Equation (2) [22,23].

$$Q = \frac{\pi}{8\eta} \left[\frac{L(1-\nu^2)(P_f - \sigma_n)}{E} \right]^3 \Delta P \quad (2)$$

In the formula:

Q is flow rate due to the pressure gradient, m^3/s ;

η is the fluid viscosity coefficient, $Pa \cdot s$;

L is the length of the fracture perpendicular to the flow direction, m ;

ν is Poisson's ratio;

P_f is the fluid pressure on the fracture surface, Pa ;

σ_n is the normal stress on the fracture surface, Pa ;

E is the Young's modulus of the rock, Pa ;

ΔP is the pressure gradient, Pa/m .

From Equation (2), it can be seen that the fluid flow rate inside the fracture surface is proportional to the cube of the fracture extension length. Since the natural fracture length is generally greater than that of the hydraulic fracture, once the hydraulic fracture communicates with the natural fracture during the fracturing process, the fracturing fluid will first leak along the natural fracture and induce fracture slippage. Further analysis shows that during the process of fluid leakage along the fracture, the fracturing fluid gathers at the perforation interval, where it communicates with the fracture, forming a pressure-drop funnel. If temporary plugging balls and temporary plugging agents are injected into the wellbore at this time for temporary plugging, they will block the high-permeability leakage channel of the fracturing fluid towards the fracture, reducing the risk of fracture slippage and subsequently reducing the risk of casing deformation, as shown in Figure 10.

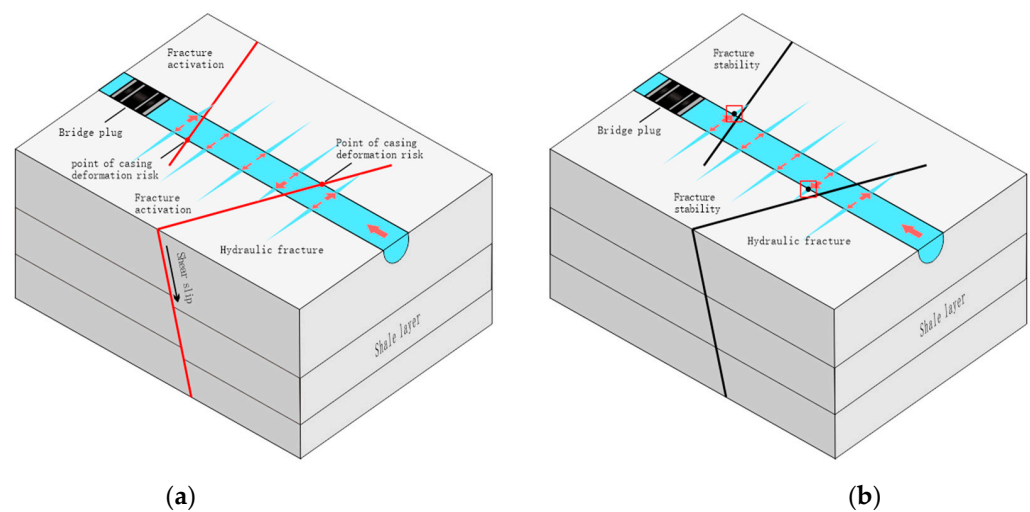


Figure 10. Casing deformation control technology of a fracturing temporary plug: (a) fracture activation for no fracturing temporary plug; (b) fracture stability for fracturing temporary plug.

3.1.2. Theory Analysis of Fracture Pumping Rate Optimization in Hydraulic Fracturing

From the analysis of Equation (1), it can be concluded that the risk of fracture slippage is influenced by the fracture geometry, geostress field, and fluid pressure within the fracture plane. The first two geological parameters remain constant in the short term, so the risk of fracture slippage is primarily controlled by the fluid pressure within the fracture plane. During the hydraulic fracturing process, the communication between the hydraulic fracture and the natural fracture result in an increase in fluid pressure within the fracture plane, thereby increasing the risk of fracture slippage. The pressure within the hydraulic fracture is closely related to the fracturing pumping rate. Generally, the pressure within the fracture increases with an increase in the pumping rate. Therefore, the risk of fracture slippage is positively correlated with the pumping rate, providing a theoretical basis for reducing the risk of casing deformation by reducing the pumping rate during the hydraulic fracturing process.

3.1.3. Fracturing Temporary Plugging Timing and Pumping Rate Optimization

According to the analysis of the casing deformation mechanism, the key to casing deformation prevention and control is to control fracture slippage. However, it is difficult to ensure that the fracture will not slip completely after communication with the hydraulic fractures during the fracturing process. However, it is possible to control the amount of slippage of the fracture by controlling the fluid volume entering the fracture. As long as the minimum passable diameter of the casing can still allow the bridge plug to pass after the deformation caused by fracture slippage, the safety of the fracturing operation can be guaranteed.

From the analysis of well structure, it can be concluded that the shear force generated by fracture slippage will first act on the cement sheath. The cement sheath will deform under the shear, and when it reaches the limit of deformation, the shear force will further transmit to the casing, causing its deformation. Therefore, in order to accurately control the amount of fracture slippage through timely temporary plugging during fracturing, it is necessary to determine the compressibility of the cement sheath and the minimum passable diameter of the casing under different shear slippage conditions of the fracture. To achieve this, a full-scale casing deformation simulation experiment was conducted, using a casing with the same specifications as the field, with an outer diameter of 139.7 mm, a wall thickness of 10.54 mm, and Q125-grade steel. The cement sheath had a thickness of 38 mm. A full-scale casing deformation simulation device was used to apply different shear displacements to the wellbore, simulating the effects of fracture slippage on the deformation of the cement sheath and casing. The experimental setup is shown in Figure 11.



Figure 11. Test of full wellbore shear casing simulation: (a) simulation of casing under shearing; (b) features of casing after shear deformation.

The experiment showed that the deformation of the casing was primarily controlled by fracture slippage, and the absorption of the cement sheath was minimal. When shear displacements of 20 mm, 30 mm, and 40 mm were applied, the minimum passable diameters of the casing were 100.4 mm, 92.5 mm, and 84.4 mm, respectively, as shown in Figure 12. For hydraulic fracturing, a minimum bridge plug outer diameter of 98 mm can be used to ensure that the minimum passable diameter of the casing after deformation can meet the boundary condition for bridge plug passage, and the minimum passable diameter should not be less than 102 mm. Therefore, according to the simulated experiment analysis of the shear deformation of the full-scale wellbore, the maximum allowable slippage induced by fracturing should be around 18 mm. Taking a safety factor of 1.1 into consideration, it is recommended that the maximum allowable slippage of the fracture should be 16 mm.

After defining the boundary conditions that allow for the maximum allowable fracture slippage, a numerical simulation technique was utilized to establish a reservoir model with pre-existing fractures. The study analyzed fracture slippage patterns under different fracturing parameters, providing a basis for optimizing the timing of temporary plugging and the pumping rate of fracturing. The model was divided into hexahedral grids, with a fracture length of 800 m. The formation was simplified as homogeneous and isotropic,

and the Von Mises yield criterion was adopted, as is shown in Figure 13, and the model parameters are listed in Table 3. The simulation results are shown in Figures 14 and 15. The simulation results indicated that the fracture slippage increased with an increase in the fracturing fluid volume. Under the condition of a pumping rate of $16 \text{ m}^3/\text{min}$, when the injected fluid volume reached 1000 m^3 , the fracture slippage reached approximately 16 mm, which is close to the maximum allowable fracture slippage. Theoretically, temporary plugging at this point can control the fracture slippage within an acceptable range, ensuring the smooth passage of the bridge plug during the fracturing operation. The analysis also revealed a close relationship between fracture slippage and the pumping rate during fracturing. With a fracturing injection volume of 1000 m^3 as an example, when the pumping rate increased from $14 \text{ m}^3/\text{min}$ to $18 \text{ m}^3/\text{min}$, the fracture slippage increased from 13.7 mm to 20.0 mm, as shown in Figures 14 and 15. Therefore, based on the simulation analysis, it is recommended to implement temporary plugging during fracturing, with a fluid volume of 1000 m^3 , and reduce the pumping rate to below $16 \text{ m}^3/\text{min}$. In the Gulong shale oil test area, two wells reduced the pumping rate from $20 \text{ m}^3/\text{min}$ to $16 \text{ m}^3/\text{min}$ in the risk section for predicting casing deformation, and temporary plugging measures were implemented. There was no casing deformation observed after fracturing, thereby verifying the effectiveness of the casing deformation prevention measures. However, it should be noted that the numerical simulation of the fracture slippage induced by hydraulic fracturing is still an idealized model which simplifies the complex geological and engineering parameters underground. Therefore, the optimization of the temporary plugging timing and pumping rate still requires validation through field experiments and continuous improvement.

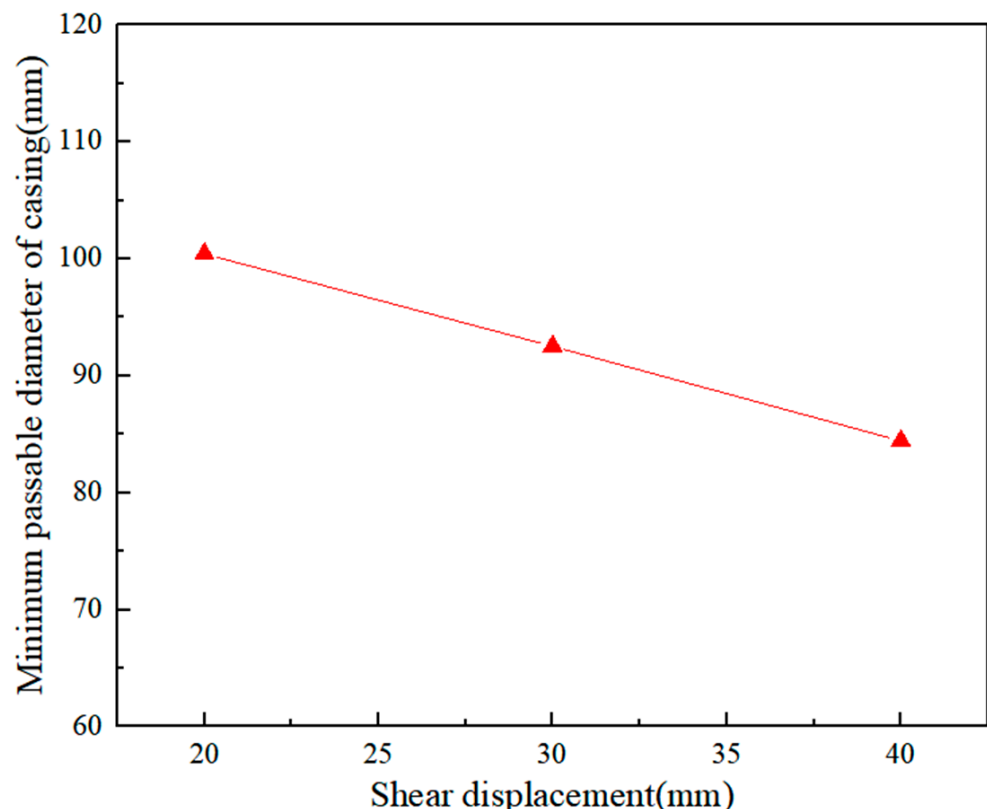


Figure 12. Variation in the minimum passable diameter of the casing with shear displacement.

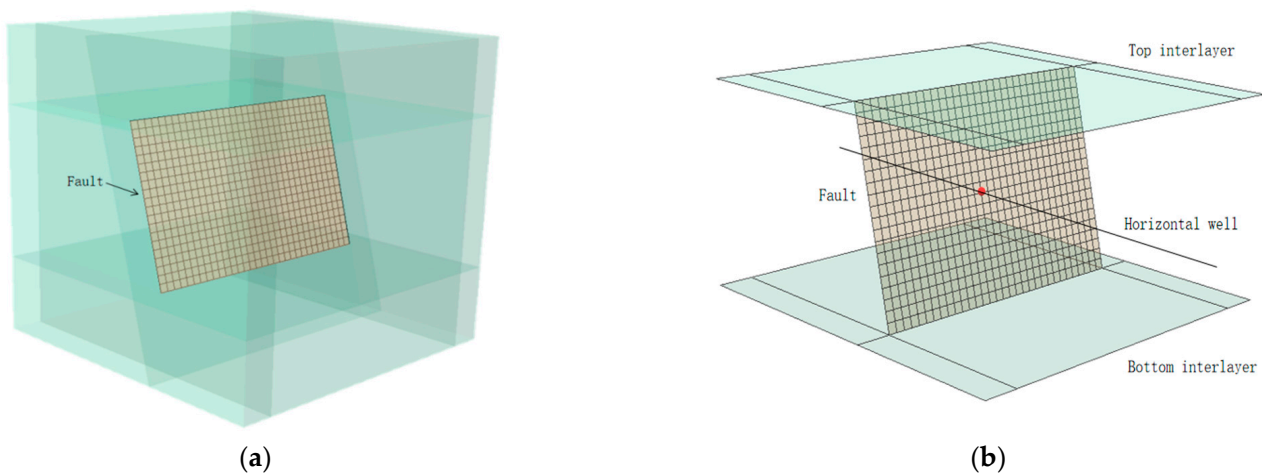


Figure 13. Numerical simulation model of fracture slip induced by hydraulic fracturing: (a) global model of fault and stratum; (b) partial amplification of fracture model.

Table 3. The parameters of the simulation model.

Parameters of Rock	
Young's modulus	20 GPa
Poisson's ratio	0.2
Parameters of fracture surface	
Length	800 m
Dip	75°
Cohesion	1 MPa
Parameters of hydraulic fracturing	
Pumping rate	14~18 m ³ /min
Injection volume	250~2000 m ³
Viscosity	2 mP.s

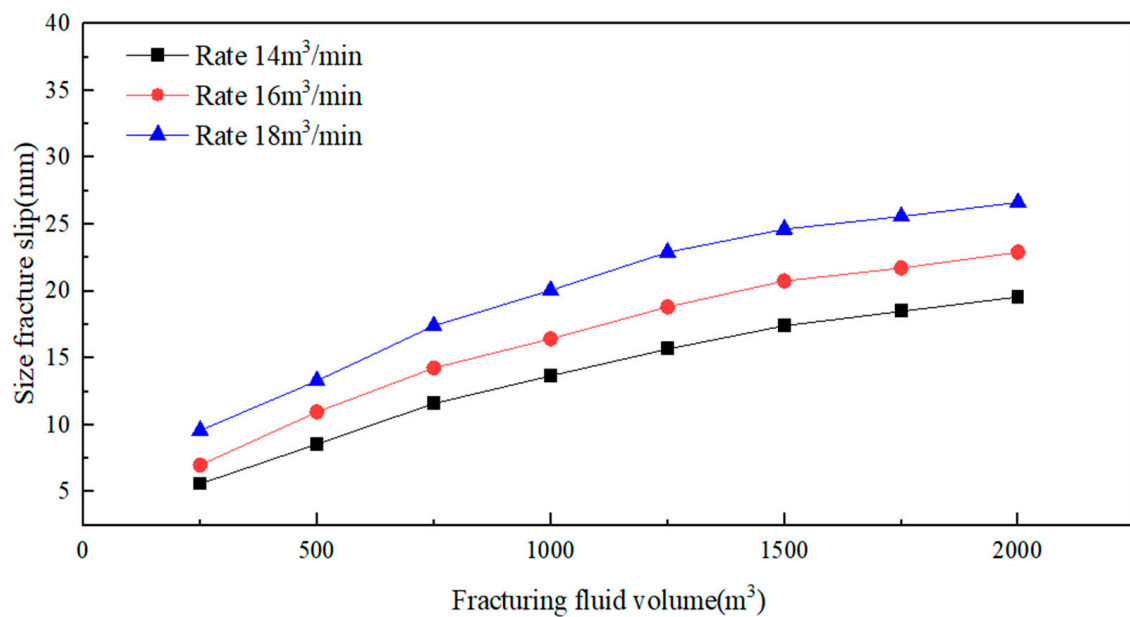


Figure 14. Variation in fracture shear slip under different fracturing parameters.

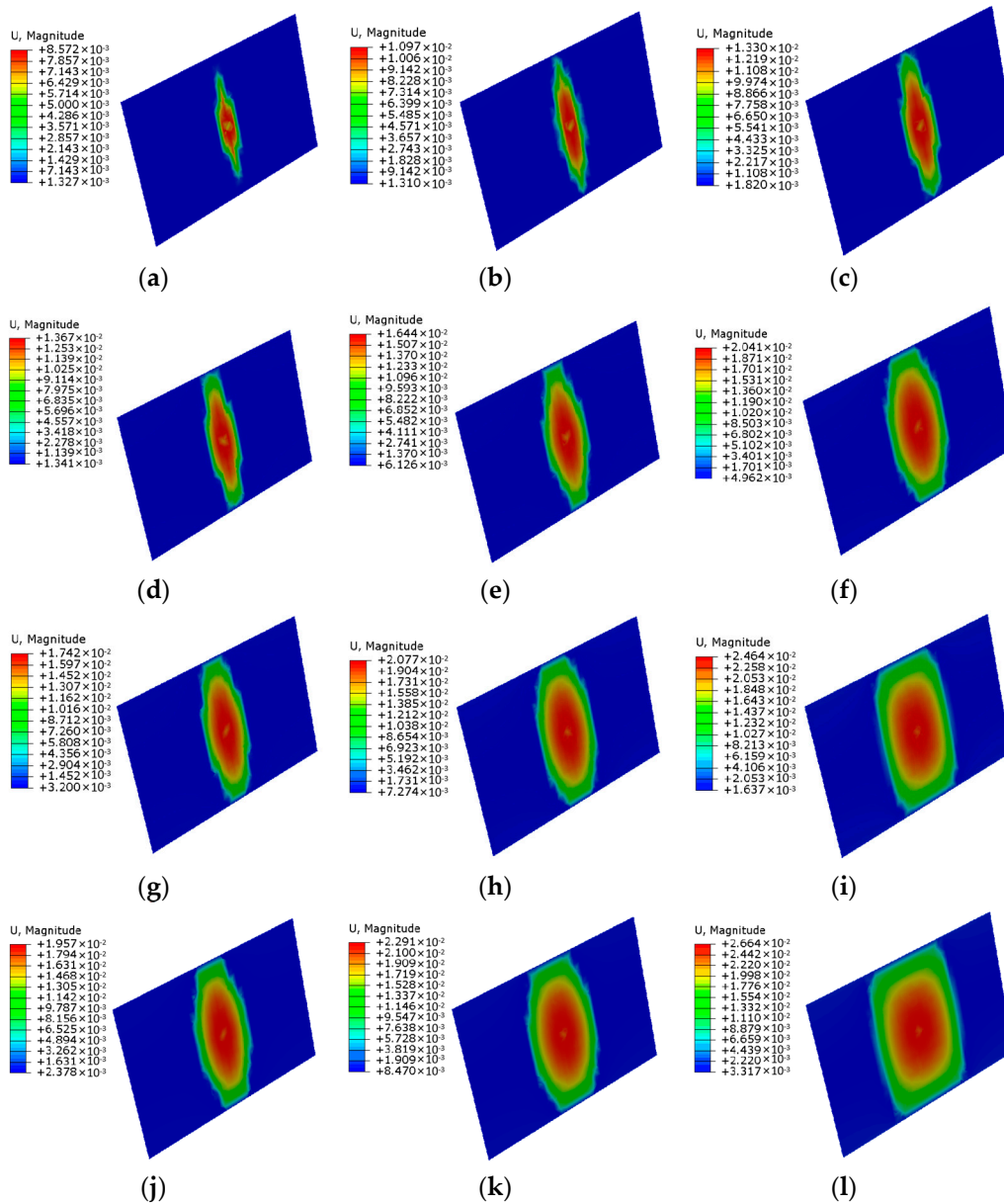


Figure 15. Numerical simulations of fracture shear slip under different fracturing parameters: (a) pumping rate $14 \text{ m}^3/\text{min}$, injected volume 500 m^3 ; (b) pumping rate $16 \text{ m}^3/\text{min}$, injected volume 500 m^3 ; (c) pumping rate $18 \text{ m}^3/\text{min}$, injected volume 500 m^3 ; (d) pumping rate $14 \text{ m}^3/\text{min}$, injected volume 1000 m^3 ; (e) pumping rate $16 \text{ m}^3/\text{min}$, injected volume 1000 m^3 ; (f) pumping rate $18 \text{ m}^3/\text{min}$, injected volume 1000 m^3 ; (g) pumping rate $14 \text{ m}^3/\text{min}$, injected volume 1500 m^3 ; (h) pumping rate $16 \text{ m}^3/\text{min}$, injected volume 1500 m^3 ; (i) pumping rate $18 \text{ m}^3/\text{min}$, injected volume 1500 m^3 ; (j) pumping rate $14 \text{ m}^3/\text{min}$, injected volume 2000 m^3 ; (k) pumping rate $16 \text{ m}^3/\text{min}$, injected volume 2000 m^3 ; (l) pumping rate $18 \text{ m}^3/\text{min}$, injected volume 2000 m^3 .

3.2. Casing Deformation Prevention Based on Cement System Optimization

According to the analysis of the mechanism of shale oil casing deformation, it is known that while controlling fracture slippage, if the compressibility of the cement sheath is high, it can effectively absorb the shear displacement caused by fracture slippage, reduce casing deformations, and ensure that the minimum remaining diameter of the casing meets the requirements for the bridge plug to pass. Based on the analysis of the multi-arm caliper logging and bridge plug resistance data, the deformations of the casings in the Gulong shale oil wells were mainly less than 25 mm, accounting for 88.6%, as shown in Figure 16.

Combining the results of the full wellbore shear casing deformation simulation experiment and Formula (3), it can be concluded that the induced fracture slippage in the Gulong shale oil wells was mainly less than 30 mm. Taking a fracture slippage of 30 mm, a casing outer diameter of 139.7 mm, and a wall thickness of 10.54 mm as the analysis conditions, in order to ensure the passage of a bridge plug with a diameter of 98 mm, which leaves a minimum remaining diameter of 102 mm for the casing, the amount of fracture slippage absorbed by the cement sheath should be no less than 17 mm after the optimization of the cementing system.

$$C_{\min} = D_c - S_f + A_c \quad (3)$$

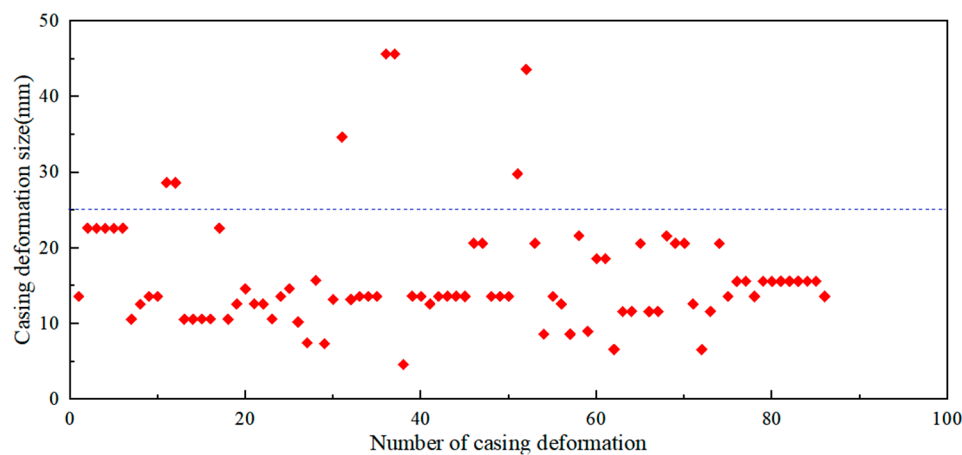


Figure 16. Size of casing deformations of Gulong shale oil wells.

In the formula:

C_{\min} is the minimum passable diameter of the casing, mm;

D_c is the inner diameter of the casing, mm;

S_f is the displacement of the fracture slip, mm;

A_c is the absorption of the cement sheath to the fracture slip, mm.

Generally speaking, the lower the elastic modulus of the cement sheath, the better the compressibility of the cement sheath. However, studies have shown that even with a lower elastic modulus, the compressibility of the cement sheath is still relatively small [24]. Moreover, it is not possible to infinitely decrease the elastic modulus of the cement sheath. Therefore, simply reducing the elastic modulus of the cement sheath is not enough to meet the requirements of absorbing the fracture slip. In order to improve the compressibility of the cement sheath, an innovative approach has been proposed to modify the cement sheath by adding high-strength hollow particles to it, thereby enhancing the compaction effect of the cement sheath. The high-strength hollow particles are composed of glass material and have diameters of about 50 μm . They can ensure that the hollow particles do not break during the expansion deformation of the casing during the fracturing process. However, when fracture slip causes shear pressure on the cement sheath, the local hollow particles will break, providing compressible space and effectively transferring excessive deformation of the casing caused by fracture slip. Obviously, the content of hollow particles in the cement sheath affects its compressibility, compressive strength, and other properties. In order to determine the appropriate content of hollow particles in the cement sheath for Gulong shale oil wells, full-scale shear simulation experiments were conducted to analyze changes in the shear displacement absorption of the cement sheath under different hollow particle content conditions. Scanning electron microscopy (SEM) analysis was also conducted on the microstructure of the cement sheath before and after the experiment. The experiment showed that the hollow particles added to the cement sheath before shear

action were relatively intact, while a large number of hollow particles were broken at the sheared area after the experiment, as shown in Figure 17.

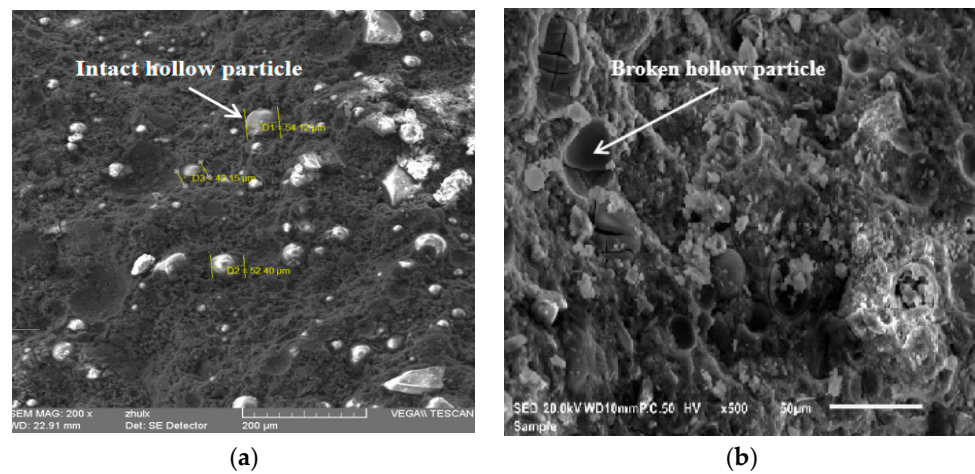


Figure 17. Morphology of hollow particles before and after the shear test of modified cementing cement: (a) morphology of hollow particles before shear compression; (b) morphology of hollow particles after shear compression.

The analysis of the experimental results showed that with the increase in the hollow particle content in the cement sheath, the shear displacement absorption capacity of the cement sheath gradually increased. When a shear displacement of 30 mm was applied, the shear displacement absorption of the cement sheath increased from 3.9 mm to 20.9 mm as the hollow particle mass ratio increased from 0 to 20%, as shown in Figure 18. When the hollow particle mass ratio was 15%, the cement sheath was able to absorb up to 17.1 mm of displacement. The minimum passable diameter of the casing was 105.7 mm, which met the requirements for the passage of bridge plugs in the field. At the same time, the compressive strength, fluid loss, and thickening time of the modified cement slurry were tested and analyzed based on relevant standards. The test results showed that the modified cement had all the required properties, including compressive strength, fluid loss, and thickening time, which met the industry standards and were suitable for field application. Based on the above analysis, it is recommended to use modified cement slurry with a hollow particle mass ratio of 15% for cementing in the Gulong shale oil wells. This will enable the cement sheath to absorb the fracture slippage caused by fracturing, transfer excessive deformation of the casing, and reduce the risk of casing failure, thus ensuring the safety of the fracturing.

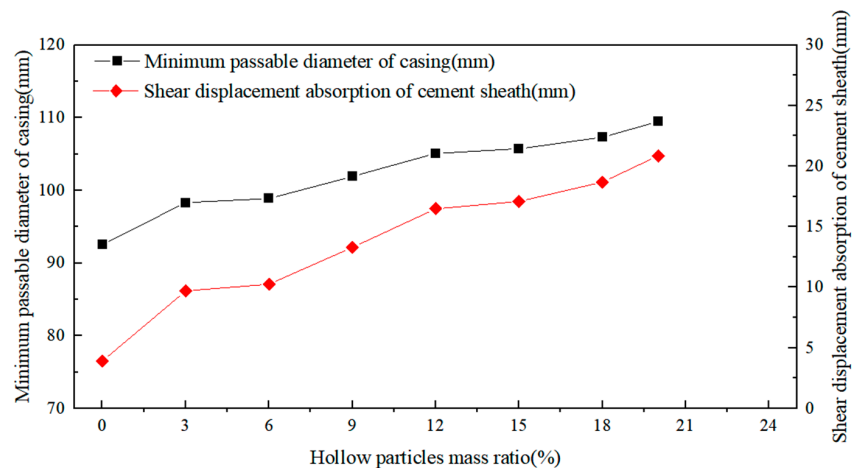


Figure 18. Variation in the minimum passable diameters of the casing and the absorption of the cement sheath with different hollow particle contents after shear tests.

4. Conclusions

Factors such as casing strength, cementing quality, and wellbore curvature have a relatively small impact on the casing deformation risk during shale oil well hydraulic fracturing. The mechanism of casing deformation is that the fluid pressure in the fracture plane increases after communication between the hydraulic fracture and pre-existing fractures, which induces the formation to slip along the fracture and then causes casing deformation under the shear action. Based on the understanding of the casing deformation mechanism, controlling the fluid pressure within the pre-existing fracture plane to reduce the slip risk is key to preventing casing deformation during shale oil well hydraulic fracturing. Temporary blocking and reducing the pumping rate during the fracturing process can block the communication pathway between hydraulic fractures and pre-existing fractures, thus controlling the fluid pressure within the fracture plane and effectively reducing the casing deformation risk. In the meantime, optimization of the cement system by adding hollow particles can effectively improve the compressive effect of the cement sheath, transfer excessive casing deformation caused by a fracture shear slip, and reduce the casing deformation risk. This provides a new method for preventing and controlling the casing deformation risk in shale oil wells. We suggest conducting on-site experiments to further verify the effectiveness of modified cement in preventing casing deformations during well cementing.

This article clarifies the mechanism of casing deformation in shale oil and proposes targeted prevention and control measures. These research findings have important reference significance for the risk prediction and prevention of casing deformation in shale oil and similar unconventional reservoirs during hydraulic fracturing.

Author Contributions: Write Original Draft Preparation, N.Z.; Methodology, P.W.; Conceptualization, J.L.; Conceptualization, W.M.; Methodology, X.Z.; Methodology, H.Z.; Methodology, C.J.; Methodology, W.H.; Data Curation, X.F.; Investigation, S.L. All authors have read and agreed to the published version of the manuscript.

Funding: This research received no external funding.

Data Availability Statement: Not applicable.

Conflicts of Interest: The authors declare no conflict of interest.

References

1. Xi, Y.; Li, J.; Liu, G.H.; Zeng, Y.J.; Li, J.P. Overview of Casing Deformation in Multistage Fracturing of Shale Gas Horizontal Wells. *Spec. Oil Gas Reserv.* **2019**, *26*, 1–6.
2. Li, J.; Ding, S.D.; Han, L.H.; Tao, Q. Research progress in failure mechanism and control methods of wellbore integrity during multi-stage fracturing of shale gas. *Pet. Tubul. Goods Instrum.* **2020**, *48*, 126–134.
3. Zhang, L.P.; Du, J.L.; Tian, Z.H.; Xu, W.L.; Zhao, Y.F.; Aliyaha, A.S.L.B.K.; Zhang, Y. Application of Seismic-Based Casing Deformation Prediction Technology in Xinjiang Oil Field. *Xinjiang Oil Gas* **2022**, *18*, 86–91.
4. Jiang, K.; Li, Q.; Chen, Y.L.; Guo, X.L.; Fu, Y.Q.; Li, J. Influence of cementing quality on casing failures in horizontal shale gas wells. *Nat. Gas Ind.* **2015**, *35*, 77–82.
5. Yu, H.; Lian, Z.H.; Lin, T.J. Numerical simulation of influence of cementing quality on casing failure for oil field. *Comput. Simul.* **2014**, *31*, 161–164.
6. Wu, J.Z.; Zhang, X.J.; Li, J.; Zhang, H.; Lian, W.; Liu, P.L. Influence of In-situ Stress Variation on Casing Load During Multi-stage Fracturing of Shale Gas Wells. *Pet. Tubul. Goods Instrum.* **2022**, *8*, 23–29.
7. Lian, Z.H.; Yu, H.; Lin, T.J.; Guo, J.H. A study on casing deformation failure during multi-stage hydraulic fracturing for the stimulated reservoir volume of horizontal shale wells. *J. Nat. Gas Sci. Eng.* **2015**, *23*, 538–546. [[CrossRef](#)]
8. Fan, M.T.; Li, J.; Liu, G.H.; Chen, X.X. Study on Casing Damage Mechanism in volume Fracturing of Shale Gas Horizontal Well. *Pet. Mach.* **2018**, *46*, 82–87.
9. Tian, Z.L.; Shi, L.; Qiao, L. Research of and countermeasure for wellbore integrity of shale gas horizontal well. *Nat. Gas Ind.* **2015**, *35*, 70–76.
10. Gao, L.J.; Liu, Z.L.; Qiao, L.; Zhuang, Z.; Yang, H.L. Mechanism Analysis and Numerical Simulation of Casing Failure in Hydraulic Fracturing of Shale Gas Formation. *Pet. Mach.* **2017**, *45*, 75–80.
11. Chen, Z.W.; Cao, H.; Zhou, X.J.; Gou, Q.Y.; Zhang, H.Z. Correlation between casing deformation and fracture zones in Changning shale gas block, Sichuan Basin. *Nat. Gas Explor. Dev.* **2020**, *43*, 123–130.

12. Chen, Z.W.; Xiang, D.G.; Zhang, F.S.; An, M.K.; Yin, Z.R.; Jiang, Z.Y. Fault slip and casing deformation caused by hydraulic fracturing in Chang-ning-Weiyuan Blocks, Sichuan: Mechanism and prevention strategy. *Pet. Sci. Bull.* **2019**, *4*, 364–377.
13. Li, L.W.; Wang, G.C.; Lian, Z.H.; Zhang, L.; Mei, Y.; He, Y.L. Deformation mechanism of horizontal shale gas well production casing and its engineering solution: A case study on the Huangjinba Block of the Zhaotong National Shale Gas Demonstration Zone. *Nat. Gas Ind.* **2017**, *37*, 91–99.
14. Zhang, F.S.; Yin, Z.R.; Chen, Z.W.; Shawn, M.; Zhang, L.Y.; Wu, Y.H. Fault reactivation and induced seismicity during multi-stage hydraulic fracturing: Field microseismic analysis and geomechanical modeling. *SPE J.* **2020**, *25*, 692–711. [[CrossRef](#)]
15. Liu, W.; Tao, C.Z.; Wan, Y.Y.; Chi, X.M.; Li, Y.; Lin, H.; Deng, J.G. Numerical analysis of casing deformation during massive hydraulic fracturing of horizontal wells in a tight-oil reservoir. *Pet. Sci. Bull.* **2017**, *4*, 466–477.
16. Fan, Y.; Huang, R.; Zeng, B.; Chen, Z.W.; Zhou, X.J.; Xiang, D.G.; Song, Y. Fault slip induced by hydraulic fracturing and risk assessment of casing deformation in the Sichuan Basin. *Pet. Sci. Bull.* **2020**, *5*, 366–375.
17. Chen, Z.W.; Fang, C.; Yong, Z.; Xiang, D.G. Deformation Characteristics and Stress Modes of Casings for Shale Gas Wells in Sichuan. *China Pet. Mach.* **2020**, *48*, 126–134.
18. Twiss, R.J.; Moores, E.M. *Structural Geology*; Freeman and Company: New York, NY, USA, 1992; p. 532.
19. Jaeger, J.C.; Cook, N.G.W. *Fundamentals of Rock Mechanics*, 3rd ed.; Chapman and Hall: London, UK, 1979; p. 593.
20. Tong, H.M.; Wang, J.J.; Zhao, H.T.; Li, B.; Hao, H.W.; Wang, M.Y. “Molar space” and its application to prediction of activity of pre-existing structures. *China Sci. Earth Sci.* **2014**, *44*, 1948–1957.
21. Tong, H.M.; Zhang, P.; Zhang, H.X.; Liu, Z.P.; Ren, X.H.; Xiao, K.Z.; Zhou, Y.B.; Deng, C. Geomechanical mechanisms and prevention countermeasures of casing deformation in shale gas horizontal wells. *Nat. Gas Ind.* **2021**, *41*, 189–197.
22. ZOBACK, M.D. *Reservoir Geomechanics*; Cambridge University Press: Cambridge, UK, 2007.
23. Tong, H.M.; Liu, Z.P.; Zhang, H.X.; Zhang, P.; Deng, C.; Ren, X.H.; Xiao, K.Z.; Zhou, Y.B. Theory and method of temporary macrofracture plugging to prevent casing deformation in shale gas horizontal wells. *Nat. Gas Ind.* **2021**, *41*, 92–100.
24. Zhang, F.S.; Jiang, Z.Y.; Chen, Z.W.; Yin, Z.R.; Tang, J.Z. Hydraulic fracturing induced fault slip and casing shear in Sichuan Basin: A multi-scale numerical investigation. *J. Pet. Sci. Eng.* **2020**, *195*, 107797. [[CrossRef](#)]

Disclaimer/Publisher’s Note: The statements, opinions and data contained in all publications are solely those of the individual author(s) and contributor(s) and not of MDPI and/or the editor(s). MDPI and/or the editor(s) disclaim responsibility for any injury to people or property resulting from any ideas, methods, instructions or products referred to in the content.